

## Exploring writhe in supercoiled minicircle DNA

This article has been downloaded from IOPscience. Please scroll down to see the full text article.

2006 J. Phys.: Condens. Matter 18 S145

(<http://iopscience.iop.org/0953-8984/18/14/S01>)

View [the table of contents for this issue](#), or go to the [journal homepage](#) for more

Download details:

IP Address: 129.252.86.83

The article was downloaded on 28/05/2010 at 09:20

Please note that [terms and conditions apply](#).

## Exploring writhe in supercoiled minicircle DNA

Jonathan M Fogg<sup>1,2</sup>, Natalia Kolmakova<sup>3</sup>, Ian Rees<sup>4</sup>, Sergei Magonov<sup>5</sup>,  
Helen Hansma<sup>3</sup>, John J Perona<sup>2</sup> and E Lynn Zechiedrich<sup>1,4</sup>

<sup>1</sup> Department of Molecular Virology and Microbiology, Baylor College of Medicine, Houston, TX 77030, USA

<sup>2</sup> Department of Chemistry and Biochemistry, University of California at Santa Barbara, Santa Barbara, CA 93106, USA

<sup>3</sup> Department of Physics, University of California at Santa Barbara, Santa Barbara, CA 93106, USA

<sup>4</sup> Program in Structural and Computational Biology and Molecular Biophysics, Baylor College of Medicine, Houston, TX 77030, USA

<sup>5</sup> VEECO Instruments, 112 Robin Hill Road, Goleta, CA 93117, USA

E-mail: [elz@bcm.edu](mailto:elz@bcm.edu)

Received 19 October 2005

Published 24 March 2006

Online at [stacks.iop.org/JPhysCM/18/S145](http://stacks.iop.org/JPhysCM/18/S145)

### Abstract

Using  $\lambda$ -Int recombination in *E. coli*, we have generated milligram quantities of supercoiled minicircle DNA. Intramolecular Int recombination was efficient down to lengths  $\sim 254$  bp. When nicked and religated in the presence of ethidium bromide, 339 bp minicircles adopted at least seven unique topoisomers that presumably correspond to  $\Delta Lk$  ranging from 0 to  $-6$ , which we purified individually. We used these minicircles, with unique  $\Delta Lk$ , to address the partition into twist and writhe as a function of  $\Delta Lk$ . Gel electrophoresis and atomic force microscopy revealed progressively higher writhe conformations in the presence of 10 mM  $\text{CaCl}_2$  or  $\text{MgCl}_2$ . From simplistic calculations of the bending and twisting energies, we predict the elastic free energy of supercoiling for these minicircles to be lower than if the supercoiling was partitioned mainly into twist. The predicted writhe corresponds closely with that which we observed experimentally in the presence of divalent metal ions. However, in the absence of divalent metal ions only limited writhe was observed, demonstrating the importance of electrostatic effects on DNA structure, when the screening of charges on the DNA is weak. This study represents a unique insight into the supercoiling of minicircle DNA, with implications for DNA structure in general.

(Some figures in this article are in colour only in the electronic version)

### 1. Introduction

The linking number ( $Lk$ ) of a DNA molecule is the number of times the two helical strands are linked together. For a relaxed molecule,  $Lk$  is approximately equal to the number of base pairs

(bp) divided by 10.5, the period of the DNA helix, and is termed  $Lk_0$ . For a closed, circular molecule  $Lk$  is, by necessity, an integer. However, almost all DNA *in vivo* has an  $Lk$  value lower than that for  $Lk_0$ . This negative linking difference,  $\Delta Lk$ , can be defined by  $\Delta Lk = Lk - Lk_0$ . Commonly, this difference is scaled to the size of the DNA by dividing by  $Lk_0$  to give the superhelical density ( $\sigma$ ) =  $\Delta Lk/Lk_0$ . Changes in the linking number are accommodated either by over-winding or under-winding of the DNA helix (twist,  $Tw$ ), or by the helix coiling upon itself (writhe,  $Wr$ ). The property  $Tw$  describes how the individual strands coil around each other along the helical axis, and is equal to  $Lk$  for a relaxed DNA molecule. The property  $Wr$  describes the coiling of the helical axis in space. These real-valued, geometric properties are related to the linking number by the equation  $Lk = Tw + Wr$ . Any change in  $Lk$  can thus be manifested as a change in  $Tw$  and/or  $Wr$  such that  $\Delta Lk = \Delta Tw + \Delta Wr$ .

The relative proportions of  $Tw$  and  $Wr$  depend on the torsional and bending rigidities of the DNA respectively, assuming a smooth untwisting or writhing regime. These properties have been measured by a number of methods. One of the most popular is measuring the cyclization efficiencies of linear DNA fragments, 200–350 bp in length (Shore *et al* 1981, Shore and Baldwin 1983, Horowitz and Wang 1984). At lengths <300 bp, the rigidity of a typical DNA helix prevents it being easily bent into a circle. The ring-closure probability, or the  $J$ -factor, (Jacobson and Stockmayer 1950), is measured from the ratio of the rates of cyclization and bimolecular association. Measured in units of concentration, the  $J$ -factor is the effective concentration of a DNA end in the vicinity of the other end, in an appropriate angular and torsional orientation for ligation. Any deformation required to align the ends should manifest as twist. Therefore, comparison of the ratios of topoisomers produced, differing by an  $Lk$  of 1, provides a measure of the torsional rigidity of the DNA (Horowitz and Wang 1984).

DNA flexibility is normally described by the persistence length, which is the length scale over which the direction of the ends are correlated. The persistence length has a value of  $\sim 150$  bp (Hagerman 1988). After two persistence lengths the correlation is lost, with an average deflection angle of  $90^\circ$ . This value, equal to two persistence lengths, is known as the Kuhn statistical length. Writhing requires a bending motion of the DNA helix. As the DNA circle length approaches the persistence length, it follows that there should be increased resistance to the introduction of  $Wr$ . However, Levene and Crothers (1986) showed that ignoring the writhe component, even in small DNA circles, leads to an underestimate of the torsional stiffness of the helix. From Monte Carlo simulations, they determined that the  $Wr$  contribution, though small, is not negligible. A theory of the dependence of  $\Delta Wr$  on  $\Delta Lk$  for minimum energy configurations of DNA minicircles was developed by Coleman *et al* (2000), for DNA treated as a classical elastic rod.

Cloutier and Widom (2004) recently reported that certain DNA fragments 94 bp in length were cyclized several orders of magnitude more efficiently than current DNA bending theory predicts. These unexpected results led the authors to suggest that DNA bending theory, determined for more gently bent regimes, did not extrapolate to sharply bent regimes as in 94 bp DNA circles. Vologodskii and co-workers (Du *et al* 2005) disputed the results of Cloutier and Widom, claiming that (i) the data were well explained by the traditional model of DNA bending, (ii) high cyclization efficiencies could be possible by transient appearance of sharp kinks, and (iii) there were problems with the experimental protocol employed by Cloutier and Widom, including the choice of cohesive ends and the concentration of ligase used in the experiment. The claims of Du *et al* were recently refuted (Cloutier and Widom 2005).

The controversy surrounding the flexibility of linear DNA notwithstanding, DNA in nature is rarely, if ever, relaxed to the extent that linear DNA is. Instead, as mentioned above, nearly all DNA in cells exists in a closed-circular underwound state. Tsen and Levene (1997) discovered that the flexibility of intrinsically bent A-tract sequences is different in supercoiled DNA than

for linear DNA. The free energy of supercoiling provides a driving force for DNA bending, which is manifest as  $Wr$ . In this study, we explore the upper limit of writhing in small, supercoiled DNA circles by gel electrophoresis and atomic force microscopy.

## 2. Materials and methods

### 2.1. Generation and purification of minicircle DNA

The construction of plasmids with sites for integrase-mediated site-specific recombination is described in the results section. A single colony of *E. coli* strain LZ54 (Zechiedrich *et al* 1997) transformed with the relevant recombination substrate was used to inoculate 20 ml Luria Bertani (LB) medium + 100  $\mu\text{g ml}^{-1}$  ampicillin and grown overnight in a standing culture. The overnight cultures were used to inoculate  $2 \times 1$  L LB + 100  $\mu\text{g ml}^{-1}$  ampicillin in shaker flasks, which were then grown overnight at 30 °C with shaking. Cells were harvested by centrifugation under sterile conditions, resuspended in 50 ml LB and used to inoculate 5 L of modified terrific broth medium in a New Brunswick BioFlo110 fermentor. The modified terrific broth medium consisted of 12 g tryptone, 48 g yeast extract, 30 ml glycerol, 0.1 ml antifoam 204 (Sigma), 2.32 g  $\text{KH}_2\text{PO}_4$ , and 12.54 g  $\text{K}_2\text{HPO}_4$  per litre. Ampicillin was added to a final concentration of 100  $\mu\text{g ml}^{-1}$ . Cells were grown at 30 °C. The pH was maintained at 7.0 during growth by addition of 2.5 M NaOH or 5% (v/v) phosphoric acid when needed. The dissolved oxygen concentration was maintained above 40% by agitation control. Cells were grown to mid-exponential phase, ( $A_{600} = 4$ ), at which point Int expression was induced by shifting the cultures to 42 °C for 30 min. After 30 min at 42 °C, norfloxacin was added to 30  $\mu\text{g ml}^{-1}$  to prevent decatenation by topoisomerase IV, and the cultures shifted back to 30 °C as Int is not active at 42 °C (Bliska and Cozzarelli 1987, Zechiedrich *et al* 1997). After 1 h at 30 °C, the cells were harvested by centrifugation.

The cells were resuspended in 500 ml GLED buffer (50 mM glucose, 10 mM EDTA, 25 mM Tris pH 8) and incubated with 2.5  $\text{mg ml}^{-1}$  lysozyme for 20 min at room temperature. The cells were lysed by addition of 1 L 1% SDS, 0.2 M NaOH for 5 min at room temperature after which time 750 ml 3 M potassium acetate pH 4 was added. Cell debris was removed by centrifugation and the supernatant precipitated with isopropanol. The pellet was resuspended in 120 ml TE buffer (pH 8). 120 ml 5 M LiCl was added to precipitate high molecular weight RNA which was removed by centrifugation. The supernatant was precipitated with ethanol, resuspended in 400 ml 750 mM NaCl, 0.5 mM EDTA, 50 mM MOPS pH 7.0, and treated with 100  $\mu\text{g ml}^{-1}$  RNaseA for 30 min at 37 °C and 100  $\mu\text{g ml}^{-1}$  proteinase K for 30 min more. Plasmid DNA was then isolated on QIAGEN-tip 10 000 anion-exchange columns following the manufacturer's instructions. The large circle was linearized by BamHI (New England Biolabs) in order to release the minicircle. The minicircle was then subjected to Sephacryl 5-500 gel filtration to remove the linearized large circle. Fractions containing minicircle DNA were pooled, and concentrated by butanol extraction followed by ethanol precipitation. Pure monomeric, supercoiled minicircle was isolated by preparative polyacrylamide gel electrophoresis on a 5% polyacrylamide gel, run at 120 V for ~6 h in Tris-borate buffer (90 mM Tris base, 90 mM boric acid, 10 mM  $\text{CaCl}_2$ ). DNA was eluted by a 'crush and soak' procedure, concentrated by butanol extraction, ethanol precipitated then resuspended in TE buffer.

### 2.2. Religation of nicked minicircle DNA

339 bp minicircle DNA was nicked at a single site using the nicking endonuclease Nt.BbvC I (New England Biolabs), incubated at 65 °C for 20 min to inactivate the endonuclease, extracted

with phenol/chloroform/isoamyl alcohol, ethanol precipitated then resuspended in TE buffer. 1  $\mu\text{g}$  of nicked minicircle was incubated with T4 DNA ligase (New England Biolabs) in 50 mM Tris-HCl pH 7.5, 10 mM  $\text{MgCl}_2$ , 1 mM ATP, 10 mM DTT, 25  $\mu\text{g ml}^{-1}$  BSA, in the absence or presence of ethidium bromide at the final concentrations of 0, 0.5, 1, 1.5, 2, 3, 4, 5 and 6  $\mu\text{g ml}^{-1}$  in a total volume of 200  $\mu\text{l}$ . Ligation was allowed to proceed overnight at room temperature after which the ligation was quenched by addition of EDTA. Ethidium bromide was removed by three rounds of extraction with 1-butanol. The DNA was ethanol precipitated, resuspended in TE buffer and analysed by polyacrylamide gel electrophoresis.

### 2.3. Electrophoresis of minicircle DNA

DNA samples were analysed by electrophoresis through 5% polyacrylamide gels (acrylamide/bis = 29:1) gels in Tris-borate buffer (90 mM Tris base, 90 mM boric acid) containing 10 mM  $\text{CaCl}_2$ , 10 mM  $\text{MgCl}_2$ , or 2 mM EDTA at 120 V for  $\sim 6$  h. The buffer was recirculated continuously throughout electrophoresis for the gels with 10 mM  $\text{CaCl}_2$  or 10 mM  $\text{MgCl}_2$ . The gels were stained with SYBR Gold (Molecular Probes) and analysed by fluorimaging on a Molecular Dynamics STORM 840 imaging system (Amersham) with quantification using ImageQuant software (Amersham).

### 2.4. Atomic force microscopy

Minicircle DNA was diluted to 0.5  $\mu\text{g ml}^{-1}$  in Tris-borate buffer (90 mM Tris base, 90 mM boric acid) containing 10 mM  $\text{CaCl}_2$  and incubated with poly-L-lysine (1  $\mu\text{g ml}^{-1}$ ) for 5 min. 20  $\mu\text{l}$  was deposited on freshly cleaved mica, incubated for 6 min, rinsed with 1 ml HPLC grade  $\text{H}_2\text{O}$ , dried with a jet of nitrogen gas then imaged in air using Multimode and Dimension 5000 AFMs equipped with a Nanoscope IIIa controller (Veeco Instruments, Goleta, CA). Imaging was performed using facilities at Veeco Instruments.

The AFM images were analysed using the Boxer component of the EMAN software package (<http://ncmi.bcm.tmc.edu/~stevel/EMAN/doc/> (Ludtke *et al* 1999, 2001)). All well-resolved non-aggregated minicircle images were cut out from the AFM files and placed, as judged by eye, into one of five classes, OPEN, BEAN, ONE, TWO+ or ROD. Attempts to use the automatic selection feature of the Boxer program to classify the images were unsuccessful. The classes are defined in section 3. Each of these classes was stored as an image stack in the Boxer program. The  $\Delta Lk$  of each particle was stored but not displayed during the classification to prevent bias. After all the images were classified, the minicircles in each class were categorized, according to  $\Delta Lk$ , and the number of each class in each topoisomer determined.

### 2.5. Analysis of integrase recombination efficiency

Plasmids with varying distances between the Int sites were transformed into *E. coli* strain LZ54. A single colony was used to inoculate 3 ml LB + 100  $\mu\text{g ml}^{-1}$  ampicillin and grown overnight in a standing culture. Overnight cultures were then used to inoculate 500 ml of LB + 100  $\mu\text{g ml}^{-1}$  ampicillin in shaker flasks, which were grown at 30 °C with shaking. During mid-exponential growth ( $A_{600} = 0.4$ ), Int expression was induced by shifting the cultures to 42 °C for 30 min. After 30 min at 42 °C, norfloxacin was added to 30  $\mu\text{g ml}^{-1}$  and the cultures shifted back to 30 °C to allow recombination to take place. After 1 h at 30 °C, the cells were harvested by centrifugation and plasmid DNA isolated using a QIAGEN Plasmid Midiprep kit and concentrated by ethanol precipitation. The DNA was cleaved with BamHI to linearize the

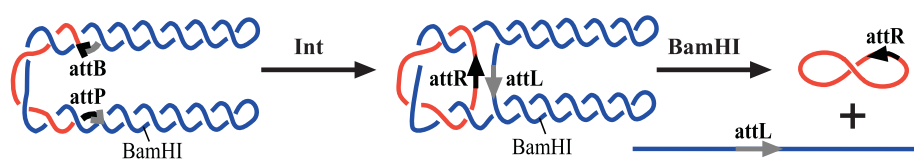


**Figure 1.** Generation of minicircle DNA by integrase-mediated site-specific recombination. Site-specific recombination between *attB* and *attP* sites, directly orientated on the same plasmid, exchanges the sequences denoted by the arrowheads, to form two catenated DNA circles. These catenanes are separated by cleavage of the large circle using BamHI, which releases the small supercoiled minicircle.

large circle and analysed by electrophoresis on a 1% agarose gel. The gels were stained with SYBR Gold and analysed by fluorimaging.

### 3. Results

#### 3.1. Integrase recombination

We used the  $\lambda$ -integrase (Int) site-specific recombination system (reviewed in Groth and Carlos (2004)) to generate minicircle DNA (figure 1). When the Int recombination sites, *attB* and *attP*, are located on the same DNA plasmid in a direct orientation, site synapsis, trapping DNA supercoil nodes, results in conversion of the plasmid into two multiply linked catenated rings (Bliska and Cozzarelli 1987). The large circle is cleaved with a restriction enzyme, BamHI, to release the supercoiled minicircle. We have used this *in vivo* system to generate milligram quantities of minicircle DNA (<500 bp).

Plasmid patt4.5D (gift from S D Levene, University of Texas, Dallas, TX), has the *attB* and *attP* sites in direct orientation separated by 1 kbp of intervening sequence. A deletion was made in patt4.5D to give a plasmid with intervening sequence 339 bp. A BbvC I restriction site was added, using a QuikChange site-directed mutagenesis kit (Stratagene), to generate a site for the Nt.BbvC I nicking endonuclease. The plasmid was transformed into *E. coli* strain LZ54 (Zechiedrich *et al* 1997). This strain has Int expression under the control of the temperature sensitive *cI* repressor. Transformants were grown at 30 °C in a New Brunswick BioFlo110 fermentor. During the exponential growth phase, the temperature was raised to 42 °C to induce expression of Int. After 30 min, to allow for expression of Int, the incubation temperature was reduced back to 30 °C to allow recombination to take place. After 1 h, the cells were harvested, lysed by alkaline lysis and minicircle DNA was isolated as described in section 2. Gel electrophoresis of minicircle DNA generated by this method revealed only three detectable topoisomers (figure 3, lane 2). The species with a  $\Delta Lk$  of  $-2$  is the predominant species (about 90%). This corresponds to a superhelical density  $\sigma = -0.07$  (assuming a helical repeat of 10.5 bp/turn), close to that in DNA isolated from *E. coli* cells (Zechiedrich *et al* 2000).

#### 3.2. Analysis of minicircle DNA topoisomers

Early studies suggested that supercoiling in DNA circles less than 500 bp is partitioned almost exclusively into untwisting of the DNA helix (Horowitz and Wang 1984). The energy required to introduce a given amount of twist per unit length of DNA should be the same irrespective of the size of the circle. Writhing, however, requires bending of the DNA helix, which becomes difficult as the length of DNA approaches the persistence length ( $\sim 150$  bp,



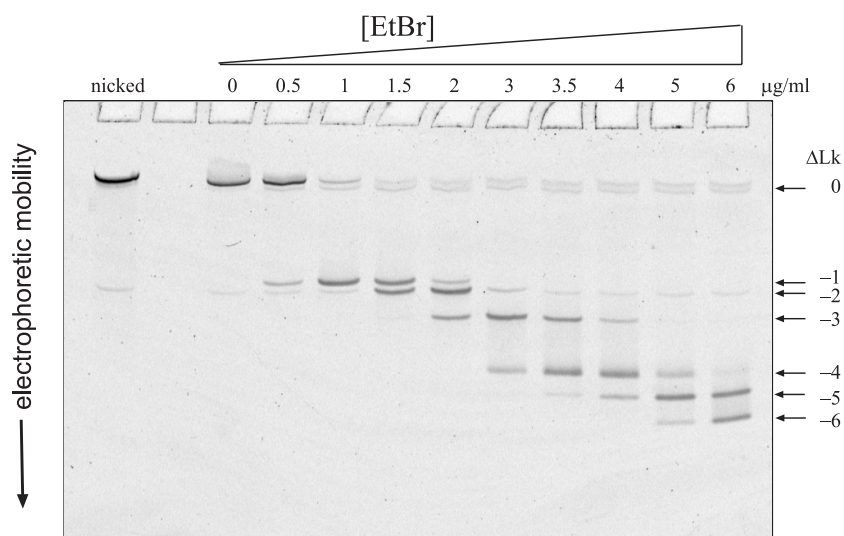


**Figure 2.** Religation of minicircle DNA in the presence of ethidium bromide. Ligation was carried out with increasing concentrations of ethidium bromide. The intercalator was extracted with butanol, and the products displayed by polyacrylamide gel electrophoresis, in the presence of 10 mM  $\text{CaCl}_2$ . No ethidium bromide was added to the gel.

(Hagerman 1988)). However, the results of Bednar *et al* (1994) suggest that in the presence of a suitable concentration of counterions, writhe may occur more readily.

A 339 bp minicircle, approximately two persistence lengths, was nicked using the nicking endonuclease Nt.BbvC I. We then religated the nick in the presence of varying concentrations of ethidium bromide, an intercalator, that causes unwinding of the DNA helix. Religation traps the unwinding, resulting in negatively supercoiled minicircle DNA. Religation requires an integral number of helical turns in order for the strand ends at the nick to be aligned. For the 339 bp minicircle, assuming a helical repeat of 10.5 bp, this requires the minicircle be unwound approximately 3/10 of a turn in order to generate the most relaxed, but covalently closed, topoisomer with a linking number of 32 ( $\Delta Lk = -0.3$ ). Although this topoisomer actually has a small amount of negative supercoiling, unlike the totally relaxed nicked minicircle, here, for simplicity, we will call this  $\Delta Lk = 0$ . Using this ligation approach, we were able to generate minicircles with linking number deficits ( $\Delta Lks$ ) ranging from 0 (with no ethidium bromide present) to what appears to be the maximal possible,  $\Delta Lk = -6$  (ligated in the presence of  $6 \mu\text{g ml}^{-1}$  ethidium bromide).

The ligation products were analysed by polyacrylamide gel electrophoresis in the presence of 10 mM  $\text{CaCl}_2$  (figure 2). As the  $\Delta Lk$  increased, the mobility of the DNA increased. Changes in twist are not thought to affect appreciably electrophoretic mobility (Bednar *et al* 1994); therefore the differences in mobility indicate conformational changes or writhing of the minicircle DNA. Nicked open-circular DNA migrates relatively slowly in the gel. The relaxed, but covalently closed ( $Lk = 32$ ), topoisomer has similar mobility, suggesting that the small amount of torsional unwinding necessary to ligate this topoisomer is partitioned almost exclusively into twist. We presume each band represents a different topoisomer with each new topoisomer differing by an  $Lk$  of one. The  $\Delta Lk$  values listed for each topoisomer are relative to the relaxed, but covalently closed ( $Lk = 32$ ), topoisomer; thus the topoisomer with  $Lk = 31$  is named  $\Delta Lk = -1$ .

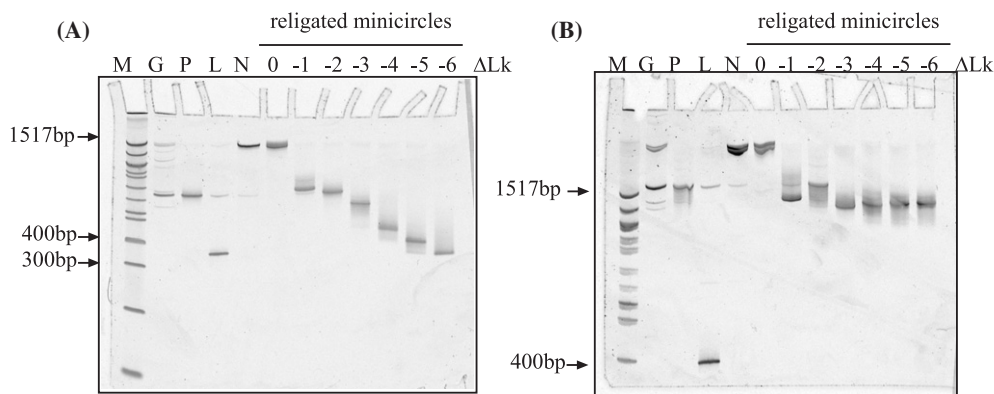


**Figure 3.** Electrophoresis of minicircle DNA in the presence of (A) 10 mM  $\text{CaCl}_2$ , or (B) 2 mM EDTA. M: 100 bp DNA ladder (NEB); G: minicircle from *in vivo* (integrase) reaction after gel filtration; P: after preparative gel electrophoresis; L: minicircle linearized by NdeI; N: minicircle nicked by Nt.BbvC I; lanes 6–12: topoisomers of minicircle, generated by religation of nicked minicircle and purified by preparative gel electrophoresis.

The removal of one helical turn results in a large increase in electrophoretic mobility, suggesting a large conformational change in the DNA, possibly a flip into a writhed figure-eight conformation. The transition from  $\Delta Lk = -1$  to  $-2$  causes only a minor additional change in mobility. This suggests that either this increase in superhelical density is manifested almost exclusively as twist, with a small amount of writhe, or that it adopts a different conformation that has nearly the same amount of compaction. It is also possible that there is some local untwisting of a short susceptible sequence of the circle, which occurs in the  $\Delta Lk = -2$  topoisomer, but not the  $\Delta Lk = -1$  topoisomer. An alternative explanation is that there is a structural transition at this superhelical density, such as strand melting or cruciform extrusion with a corresponding reduction in writhing (Nordheim and Meese 1988). The *attR* site on the minicircle is AT rich and thus may be more susceptible to localized untwisting or even strand melting. To investigate these possibilities we probed the minicircle with the ssDNA specific nuclease, S1, and T7 endonuclease I, which is specific for branched DNA (data not shown). Preliminary data show general increased sensitivity to both enzymes with increased superhelical density in the minicircles, revealing the presence of unwound regions and possible supercoiling-dependent alternative secondary structures.

There is a large increase in mobility from  $\Delta Lk = -3$  to  $-4$ , which may indicate a transition into a very compact, highly writhed structure, perhaps a cloverleaf structure (Coleman *et al* 2000). Additional increases in  $\Delta Lk$  result in only small increases in electrophoretic mobility, suggesting minimal further alterations in writhe or conformation. The results above show that the supercoiling in small DNA circles is partitioned into both twist and writhe, and that the partition may vary for different topoisomers.

### 3.3. Importance of counterions

DNA is a highly charged molecule and therefore the likelihood that a DNA molecule can writhe, which requires two highly charged helices to juxtapose, is strongly influenced by counterions. In another paper in this issue, Randall *et al* (2006), we examine the effect of counterions on the likelihood of two DNA helices juxtaposing. Counterions shield the negative charge of the phosphates on the DNA backbone and therefore allow a close approach of DNA helices.



To study this directly, we purified individual topoisomers of 339 bp minicircle DNA by gel electrophoresis. These were then analysed by polyacrylamide gel electrophoresis in Tris-borate buffer containing either 10 mM  $\text{CaCl}_2$  (figure 3(A)) or 2 mM EDTA (figure 3(B)). The pattern of mobilities in the presence of  $\text{CaCl}_2$  is described above. The pattern of mobilities in the presence of  $\text{MgCl}_2$  was the same as for  $\text{CaCl}_2$  (data not shown). In the absence of added divalent metal ions, the pattern is very different. The transition from  $\Delta Lk = 0$  to  $\Delta Lk = -1$  on the gel with 2 mM EDTA (figure 3(B)) resembles the same transition in the presence of  $\text{CaCl}_2$  (figure 3(A)), suggesting a similar amount of writhe. However, nothing else is similar. Further increases in  $\Delta Lk$  exhibit very little change in electrophoretic mobility. This suggests that under EDTA conditions the charge on the DNA backbone prevents the helices coming any closer than that required, perhaps, for a figure-eight conformation. The  $\Delta Lk = -2$  topoisomer migrates more slowly than the less supercoiled  $\Delta Lk = -1$  topoisomer, possibly indicating a structural transition for this topoisomer that is then suppressed with additional  $\Delta Lk$ .

The type and concentration of counterions in solution is known to strongly affect the structure of supercoiled DNA. From measurements of knotting probabilities of DNA, Rybenkov *et al* (1993) and Shaw and Wang (1993) determined the effective diameter of DNA as a function of  $\text{Na}^+$  concentration. At low concentrations of counterions, the poor electrostatic screening of the phosphates resulted in an effective DNA diameter of 15 nm, several times greater than the geometric diameter of the double helix. However, at high concentrations of counterions the effective diameter approaches the physical diameter of the DNA helix (2 nm). Comparable results were observed at  $\text{MgCl}_2$  concentrations that were 10- to 50-fold lower than the corresponding NaCl concentration (Shaw and Wang 1993). It is apparent that the structure of the DNA is extremely sensitive to solution conditions.

### 3.4. Atomic force microscopy of minicircle DNA

Gel electrophoretic mobility is one way to study DNA conformation. We also analysed the different minicircle topoisomers using atomic force microscopy (AFM). Individual topoisomers were purified by polyacrylamide gel electrophoresis and analysed by AFM. The samples were prepared for AFM in the presence of  $\text{CaCl}_2$ , which allows the close approach of two helices. We also sought to mimic the conditions used in gel electrophoresis as closely as possible.

Depending upon  $\Delta Lk$ , different conformations were observed. All well-resolved non-aggregated minicircles were cut out from the micrograph images and placed, as judged by eye, into image stacks using the Boxer component of the EMAN image analysis software package. Boxed images were each categorized into one of five classes, as exemplified in figure 4(A), according to the following definitions:

OPEN: undistorted smooth circle.

BEAN: kinked or distorted helix, but no points of helix-helix contact.

ONE: one helix-helix contact point.

TWO+: at least two helix-helix points of contact, but with clear open space visible between the contact points.

ROD: compact and highly writhed, with no clear space between contact points.

Image reconstruction within each class, using EMAN, did not yield a clear averaged image. This is likely because of the flattening of the three-dimensional object into two dimensions when the DNA is immobilized on the mica. Except for OPEN and ROD, there is a large potential for overlap between the classes, depending on how the minicircle lies on the mica. Despite these drawbacks, we show that AFM is a useful technique for visualizing supercoiled minicircle DNA.

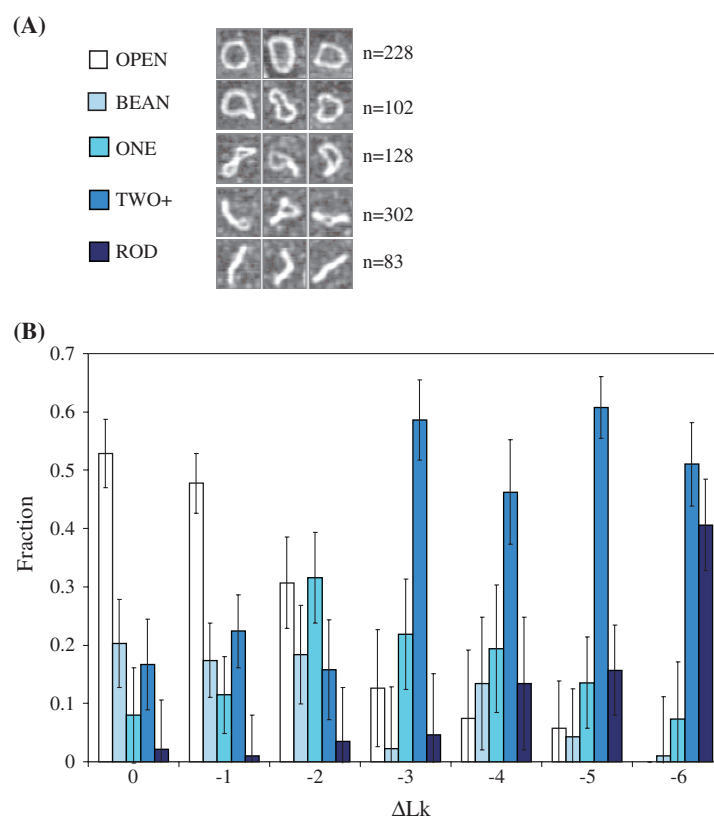


**Figure 4.** Analysis of DNA minicircles by atomic force microscopy (AFM). (A) Individual molecules were categorized into one of the five classes, OPEN, BEAN, ONE, TWO+ or ROD. Examples of each of the classes and total number of molecules in each class (over all topoisomers) are shown. (B) Relative proportions of each class as a function of  $\Delta Lk$ . The error bars were calculated according to the equation  $\sqrt{p(1-p)/n}$ , where  $p$  is the population and  $n$  is the number of molecules in the class (for each topoisomer).

A total of 843 molecules were categorized and the relative proportions of each class in each topoisomer were determined (figure 4(B)). The results clearly show an increase in the number of highly writhed conformations with increasingly negative  $\Delta Lk$ . For the relaxed topoisomer ( $\Delta Lk = 0$ ), most of the molecules were in the open form. The open circles have a diameter of approximately 35 nm, as expected for a DNA contour length of 112 nm (339 bp, 0.33 nm rise/bp). The proportion of the open-circle form decreased with increasingly negative  $\Delta Lk$ . The  $\Delta Lk = -2$  topoisomer contained a mixture of open-circular molecules, and molecules in what looks like a figure-eight conformation. At higher  $\Delta Lk$ , most of the minicircles have two or more writhes. For the hypernegatively supercoiled ( $\Delta Lk = -6$ ) topoisomer approximately half of the minicircles were RODs, with dimensions  $\sim 50 \text{ nm} \times 5 \text{ nm}$ . The RODs most likely have three or even more writhes. The AFM analysis, combined with the electrophoresis results, concurs that 339 bp circles, with counterions present, can manifest  $\Delta Lk$  into significant writhe.

### 3.5. Integrase recombination as a function of distance between sites

We used the  $\lambda$ -integrase (Int) site-specific recombination system as an *in vivo* probe for the flexibility of supercoiled DNA. A series of deletions were made in patt4.5D to give plasmids

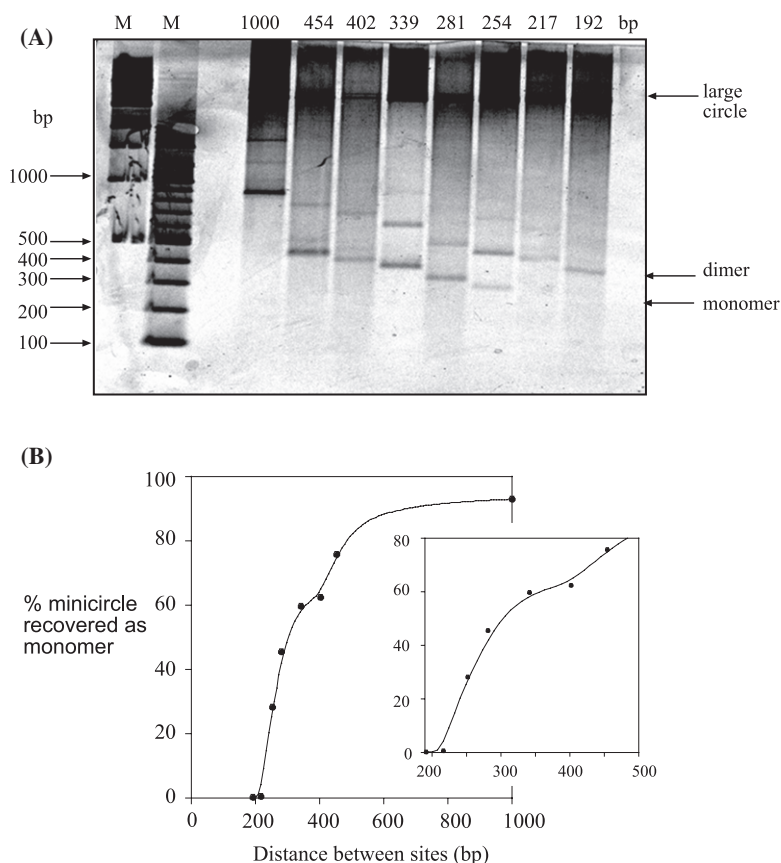


**Figure 5.** Integrase-mediated recombination efficiency as a function of distance between *attB* and *attP* sites. (A) Products of integrase recombination separated by agarose gel electrophoresis. Lane 1: 100 bp DNA ladder (NEB); lane 2: 1 kb DNA ladder (NEB); lanes 4–11: products of integrase recombination for various spacings between the *attB* and *attP* sites. (B) Efficiency of intramolecular recombination as a function of distance between *attB* and *attP* sites. Inset: efficiency of intramolecular recombination over the range 200–500 bp.

with intervening sequences, between the cleavage sites of *attB* and *attP*, of 192, 217, 254, 281, 339, 402, 454 and 1000 bp. The set of plasmids were transformed into *E. coli* strain LZ54 (Zechiedrich *et al* 1997). Transformants were grown at 30 °C in shaker flasks. During the exponential growth phase, the temperature was raised to 42 °C for 30 min to induce Int expression, then reduced back to 30 °C to allow recombination to take place. After 1 h, the cells were harvested, DNA isolated using QIAGEN midiprep kits, cleaved with BamHI to release the minicircle DNA, and analysed by gel electrophoresis (figure 5). The gel was stained with SYBR Gold and analysed by fluorimaging.

$\lambda$ -integrase recombination occurred with all substrates. However, in the cases when the intervening sequence was 192 or 217 bp, the minicircles produced were two or three times the expected size. For plasmids with a long intervening sequence, recombination occurs more readily with sites in the same plasmid than between plasmids, because of the proximity of the two Int sites. As the intervening sequence becomes shorter, it becomes progressively more difficult for the recombinase system to achieve the site synapsis necessary for recombination to take place. Therefore, in order for recombination to take place, synapsis must occur with a

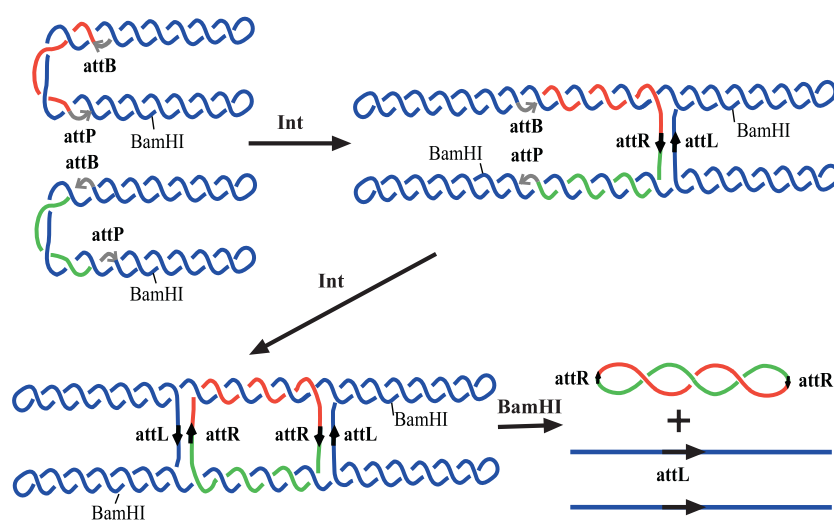


**Figure 6.** Generation of dimers by integrase recombination. Site-specific recombination between *attB* and *attP* sites on different plasmids leads to the formation of a dimer plasmid. Further recombination between the remaining *attB* and *attP* sites leads to catenane formation. Cleavage of the large circle by *BamHI* releases the minicircle DNA which is twice the size of minicircle generated by recombination between sites on the same plasmid (figure 1).

site on a different plasmid resulting in dimer formation (figure 6). The resulting dimer can then undergo further intramolecular recombination to yield a minicircle twice the size. We observed a clear inverse relationship between the length of the intervening sequence and the efficiency of intramolecular recombination (figure 5(B)). The lower than expected monomer recovery for the 402 bp minicircle may be a phasing effect caused by the helical repeat of DNA. However, we would need to investigate a series of spacings differing by only a few base pairs to conclude this.

The decreased intramolecular efficiency is most likely a result of the energetic cost of bending the short segment of intervening DNA in the cell. As the length of the intervening sequence decreases, this energetic cost becomes higher. Bimolecular recombination (i.e. between sites on different plasmids) does not require this energetic cost of DNA bending and therefore becomes energetically favourable.

### 3.6. Thermodynamics of supercoiling in small DNA circles

Horowitz and Wang (1984) and Shore and Baldwin (1983) determined the free energies of supercoiling in DNA circles as small as 210 bp. These energies were calculated from the ratios of the topoisomers generated by circularization of short linear DNAs by ligation. As a result, the energies calculated are only applicable for low values of  $\Delta Lk$ .

The free energy of supercoiling exhibits quadratic dependence on the linking difference:

$$\Delta G_{SC} = K \cdot \Delta Lk^2 \quad (1)$$

where  $K$  is a DNA length-dependent proportionality constant. For DNA rings larger than 2000 bp, Horowitz and Wang (1984) found that  $NK$  is approximately constant at approximately  $1150RT$ , where  $N$  is the number of base-pairs,  $R$  is the universal gas constant ( $8.3 \text{ J K}^{-1} \text{ mol}^{-1}$ ) and  $T$  the absolute temperature (kelvin). For rings smaller than 2000 bp, Horowitz and Wang (1984) found that  $NK$  increased steadily with decreasing  $N$ . For a 210 bp ring,  $NK$  was calculated to equal  $3900RT$ . We replotted the values of  $NK$  versus  $N$  from

Horowitz and Wang (1984), using Kaleidagraph, to estimate the free energy of the 339 bp minicircle used in this study. From the replotted curve of  $NK$  versus  $N$ , we calculated  $NK$  to be  $\sim 3650RT$ .

The free energy of supercoiling is a sum of the energies required for twisting and writhing of the DNA helix:  $\Delta G_{SC} = \Delta G_{writhe} + \Delta G_{twist}$ . The free energy for writhing the helix is given by

$$\Delta G_{writhe} = B \left( \frac{\vartheta^2}{2L} \right) \quad (2)$$

where  $L$  is the axial length of the DNA,  $\vartheta$  is the DNA bending angle (in radians) and  $B$  the bending force constant ( $=140RT$  bp at 298 K (Bates and Maxwell 2005)). Similarly, for twisting,

$$\Delta G_{twist} = C \left( \frac{\phi^2}{2L} \right) \quad (3)$$

where  $C$  is the twisting force constant ( $=180RT$  bp at 298 K (Bates and Maxwell 2005)), and  $\phi$  is the angle (in radians) through which the DNA is over or undertwisted.

It must be noted that for DNA circles of this size there is considerable bending strain even in the relaxed isomer. It is necessary to bend the DNA by  $360^\circ$  ( $2\pi$  radians) in order for the DNA to be circular (assuming that the bend is uniformly distributed with no kinks). In order to introduce one writhe, it is necessary to bend the DNA by an additional  $360^\circ$  ( $2\pi$  radians), again assuming that the bend is uniformly distributed. It is unlikely that the bend is uniformly distributed and it is more likely that there will be a greater degree of bending at the apices of the superhelix. However, for simplicity we assume uniform bending is the case. We predict that the presence of sharp kinks in the DNA, such as at the apices of the  $\Delta Lk = -6$  topoisomer, should occur at DNA sequences that are more easily bent. The free energy required for bending would then be lower than predicted here, thus making the writhed state even more favourable.

Taking the  $\Delta Lk = -2$  topoisomer as an example, if the  $\Delta Lk$  of  $-2.3$  is partitioned exclusively into twist,  $\Delta G_{SC} = \Delta G_{twist} = (90RT \text{ bp} \times (4.6\pi)^2)/339 \text{ bp} = 55.4RT$ . Substituting this value for  $\Delta G_{SC}$  into equation (1) gives a value for  $NK$  of  $3550RT$ , close to that obtained from the calculations of Horowitz and Wang.

We can predict the free energy required to introduce one writhe into the minicircle, such that  $\Delta Wr = -1$  and  $\Delta Tw = -1.3$ . The total bending energy required is given by  $\Delta G_{bend} = (70RT \text{ bp} \times (4\pi)^2)/339 \text{ bp} = 32.6RT$ . To calculate the energy from writhing we need to subtract the bending energy for a nicked minicircle;  $\Delta G_{bend} = (70RT \text{ bp} \times (2\pi)^2)/339 \text{ bp} = 8.2RT$ . Thus the writhing free energy is given by  $\Delta G_{writhe} = 32.6RT - 8.2RT = 24.4RT$ . The twisting free energy is given by  $\Delta G_{twist} = (90RT \text{ bp} \times (2.6\pi)^2)/339 \text{ bp} = 17.7RT$ . These values give  $\Delta G_{SC} = 42.1RT$ , which is significantly lower than the value calculated for an unwrithed minicircle. Substituting this value into equation (1) gives a value of  $NK$  of  $2968RT$ , lower than predicted by the results of Horowitz and Wang.

The above example demonstrates how the free energy of supercoiling decreases as the supercoiling is partitioned into writhe. We used the analysis described above to predict free energies of supercoiling for different levels of writhe of each of the seven topoisomers (figure 7). For the most relaxed, but covalently closed,  $\Delta Lk = 0$ , topoisomer, any amount of writhe is energetically unfavourable. Thus, the small amount of supercoiling required to align the strands is likely partitioned exclusively into twist. This is indeed what is observed by polyacrylamide gel electrophoresis. For the  $\Delta Lk = 0$  topoisomer it is, therefore, likely that the value for  $NK$  is closer to that derived from the results of Horowitz and Wang. However, for all other topoisomers writhe is favourable. For the hypernegatively supercoiled,  $\Delta Lk = -6$ , topoisomer the most energetically favourable conformation has approximately three writhes.

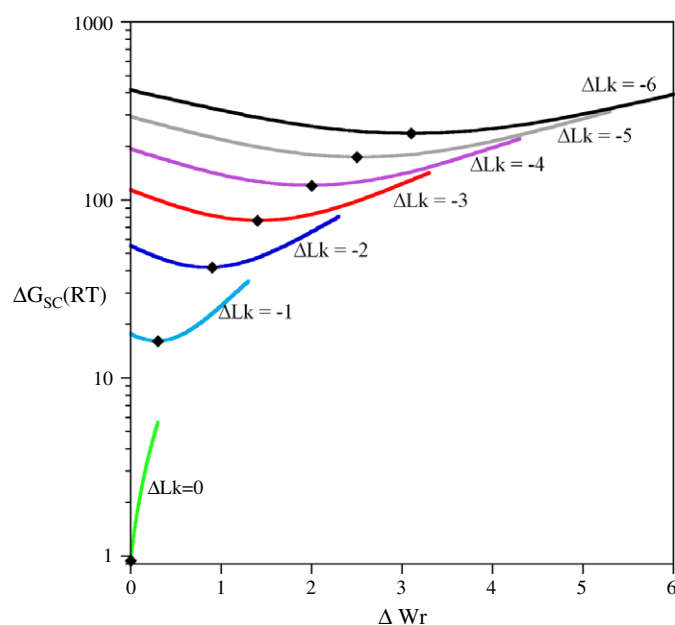


**Figure 7.** Predicted free energies for different values of writhe for each of the topoisomers of the 339 bp minicircle. Free energies were calculated as described in the text. Diamonds indicate energy minima for each topoisomer. Lowest predicted free energies occurred for  $\Delta Wr$  of 0, 0.3, 0.9, 1.4, 2.0, 2.5 and 3.1, for topoisomers  $\Delta Lk = 0, -1, -2, -3, -4, -5$  and  $-6$  respectively.

Thus, although the crossovers are not discernible in the AFM images of this topoisomer, we can predict that most likely there are three.

In the calculations above we have ignored the electrostatic contribution to the free energy of supercoiling. In the presence of a suitable concentration of counterions, in this case 10 mM  $Ca^{2+}$  (figures 3(A) and 4), the charges on the DNA phosphates are screened and thus electrostatic energy is minor in comparison to the bending and twisting energy (Schlick *et al* 1994). However, for the case with no divalent metal ions present (figure 3(B)), the electrostatic energy is likely the dominant component of the free energy of supercoiling (Schlick *et al* 1994). Additionally, recent data suggest that the bending resistance of DNA is dependent on the effective diameter of the DNA (Toan *et al* 2005). Therefore the above calculations of supercoiling free energy only apply to conditions where counterions are present.

The supercoiling free energy for writhed minicircles is lower than if the supercoiling was partitioned only into twist. Indeed, Bates and Maxwell (1989) found that DNA gyrase was able to introduce negative supercoiling into DNA circles as small as 174 bp. The free energy of supercoiling for the reaction is acquired by the hydrolysis of two ATP molecules by DNA gyrase. On the basis of the free energy calculations of Horowitz and Wang, however, the amount of free energy required for the reaction is about twice that available from the ATP hydrolysis. If we substitute our predicted values for  $\Delta G_{sc}$  into equation (1), the value for  $K$  decreases as  $-\Delta Lk$  increases. Thus, the values of supercoiling free energy calculated for minicircles at low superhelical density do not extrapolate to more negatively supercoiled regimes. We predict that supercoiling in minicircle DNA is likely to be partitioned into both twist and writhe, because the writhed state is a lower energy state. We are currently analysing the thermodynamics of supercoiling in minicircles, taking into account sequence effects, which will be the subject of a future publication.



#### 4. Discussion

We have analysed supercoiled DNA minicircles by two independent methods. DNA supercoiling was introduced by religation of nicked minicircle in the presence of an intercalator (ethidium bromide). Using this approach, we generated hyper-negatively supercoiled DNA. A linking number deficit as high as  $\Delta Lk = -6$  can be achieved for a 339 bp minicircle. The relaxed form of this minicircle should have a total of 32 helical turns (as calculated from a helical repeat of 10.5 bp/turn (Bates and Maxwell 2005)). The most supercoiled form we can achieve ( $\Delta Lk = -6$ ) has only 26 helical turns, corresponding to a superhelical density  $\sigma = -0.195$ . Increasing the ethidium bromide concentration used in the ligation beyond that described here did not result in higher  $\Delta Lks$ . There are several possible reasons for this. One likely possibility is that the DNA cannot bind any more ethidium bromide. It has been determined that  $\sim 14$  ethidium bromide molecules are required to unwind one turn (Wang 1974, Pulleyblank and Morgan 1975). Therefore a  $\Delta Lk$  of  $-6$  requires 84 ethidium bromide molecules. An alternative possibility is that the DNA cannot accommodate any more writhe. Further increases in superhelical density will not cause further increases in writhe and would not be distinguished by gel electrophoresis. Our future work will test if this is the case by electrophoresis in the presence of an intercalator.

Bednar *et al* (1994) also observed writhe in minicircle DNA. Using a 178 bp minicircle, they observed that a  $\Delta Lk$  of 1.5–2 was required to flip the minicircle into a writhed conformation, in the presence of neutralizing concentrations of counterions. For our larger 339 bp minicircle, a linking number deficit of less than one is required to induce a writhed, figure-eight conformation even in the absence of counterions. Increasing the linking number deficit results in tightly interwound, multiply writhed minicircles, but only in the presence of counterions.

From simplistic calculations of the elastic free energy we predicted the values of writhe for each of the seven topoisomers. These are in close agreement with the amount of writhe observed in the AFM images and by electrophoresis. The experimental results also agree closely with calculations for a 350 bp minicircle formed from intrinsically straight DNA (Coleman *et al* 2000). We can therefore conclude that the results are consistent with standard DNA bending theory.

In the absence of counterions, the electrostatic component must also be taken into consideration. In this case, the repulsion of charged DNA segments will prevent a close association of helices. This limits the amount of writhe than can be accommodated, even at very high  $\Delta Lks$ . It should be noted, however, that the intracellular concentration of monovalent and divalent cations in *E. coli* (Richey *et al* 1987, Record *et al* 1998), should be sufficiently high to effectively screen the charges on the phosphates. Therefore, we conclude that the highly writhed conformations we observe in the presence of counterions are the most physiologically relevant.

There is clearly a strong resistance to bending short regions of DNA as observed by the reduced efficiency of site synapsis we observe with integrase. Integrase-mediated recombination is facilitated *in vivo* by the integrase host factor (IHF), which introduces a bend of  $\sim 160^\circ$  into the DNA (Rice *et al* 1996) enabling site synapsis. However, the IHF appears to be insufficient to completely overcome the energetic cost of bending the DNA. The results with integrase represent bending of supercoiled plasmid DNA in the cell.

In summary, the combination of atomic force microscopy and gel electrophoresis presented here provides a significant insight into the understanding of supercoiled DNA. The ability to produce milligram quantities of these DNA minicircles means we are now able to perform a

broad range of biophysical analyses, which should further advance our understanding of the true higher-order structure of physiologically relevant DNA.

### Acknowledgments

We would like to thank Jennifer K Mann, De Witt L Summers, Stephen D Levene, Graham L Randall and Bernard D Coleman, for stimulating discussions, and for critically reading the manuscript. Funding was provided by the Program in Mathematics and Molecular Biology to JMF. This work was supported by NSF grant MCB-0090880, NIH grant RO1 AI054830, and the Burroughs Wellcome Fund to ELZ.

### References

- Bates A D and Maxwell A 1989 *EMBO J.* **8** 1861–6
- Bates A D and Maxwell A 2005 *DNA Topology* 2nd edn (Oxford: Oxford University Press)
- Bednar J, Furrer P, Stasiak A, Dubochet J, Egelman E H and Bates A D 1994 *J. Mol. Biol.* **235** 825–47
- Bliska J B and Cozzarelli N R 1987 *J. Mol. Biol.* **194** 205–18
- Cloutier T E and Widom J 2004 *Mol. Cell.* **14** 355–62
- Cloutier T E and Widom J 2005 *Proc. Natl Acad. Sci. USA* **102** 3645–50
- Coleman B D, Swigon D and Tobias I 2000 *Phys. Rev. E* **61** 759–70
- Du Q, Smith C, Shiffeldrim N, Vologodskaya M and Vologodskii A 2005 *Proc. Natl Acad. Sci. USA* **102** 5397–402
- Groth A C and Carlos M P 2004 *J. Mol. Biol.* **335** 667–78
- Hagerman P J 1988 *Ann. Rev. Biophys. Biochem.* **17** 265–86
- Horowitz D S and Wang J C 1984 *J. Mol. Biol.* **173** 75–91
- Jacobson H and Stockmayer W H 1950 *J. Chem. Phys.* **18** 1600–6
- Levene S D and Crothers D M 1986 *J. Mol. Biol.* **189** 73–83
- Ludtke S J, Baldwin P R and Chiu W 1999 *J. Struct. Biol.* **128** 82–97
- Ludtke S J, Jakana J, Song J L, Chuang D and Chiu W 2001 *J. Mol. Biol.* **314** 253–62
- Nordheim A and Meese K 1988 *Nucleic Acids Res.* **16** 21–37
- Pulleyblank D E and Morgan A R 1975 *J. Mol. Biol.* **91** 1–13
- Randall G L, Pettitt B M, Buck G and Zechiedrich E L 2006 *J. Phys.: Condens. Matter* **18** S173
- Record M T Jr, Courtenay E S, Cayley D S and Guttman H J 1998 *Trends Biochem. Sci.* **23** 143–8
- Rice P A, Yang S, Mizuuchi K and Nash H A 1996 *Cell* **87** 1295–306
- Richey B, Cayley D S, Mossing M C, Kolka C, Anderson C F, Farrar T C and Record M T Jr 1987 *J. Biol. Chem.* **262** 7157–64
- Rybenkov V V, Cozzarelli N R and Vologodskii A V 1993 *Proc. Natl Acad. Sci. USA* **90** 5307–11
- Schlick T, Li B and Olson W K 1994 *Biophys. J.* **67** 2146–66
- Shaw S Y and Wang J C 1993 *Science* **260** 533–5
- Shore D and Baldwin R L 1983 *J. Mol. Biol.* **170** 957–81
- Shore D, Langowski J and Baldwin R L 1981 *Proc. Natl Acad. Sci. USA* **78** 4833–7
- Toan N M, Marenduzzo D and Micheletti C 2005 *Biophys. J.* **89** 80–6
- Tsen H and Levene S D 1997 *Proc. Natl Acad. Sci. USA* **94** 2817–22
- Wang J C 1974 *J. Mol. Biol.* **89** 783–801
- Zechiedrich E L, Khodursky A B, Bachellier S, Schneider R, Chen D, Lilley D M J and Cozzarelli N R 2000 *J. Biol. Chem.* **275** 8103–13
- Zechiedrich E L, Khodursky A B and Cozzarelli N R 1997 *Genes. Dev.* **19** 2580–92